*J. Fluid Mech.* (1982), *vol.* 120, *pp.* 323–346
*Printed in Great Britain*


# Kinematic-wave theory of sedimentation beneath inclined walls

By W. SCHNEIDER
Institut für Strömungslehre und Wärmeübertragung,
Technische Universität Wien, Vienna, Austria

(Received 18 March 1981 and in revised form 20 November 1981)

The two-phase flow in settling vessels with walls that are inclined to the vertical is investigated. By neglecting inertial effects and the viscosity of the suspension it is shown that the particle concentration remains constant on kinematic-wave fronts. The wave fronts are horizontal and propagate in a quasi-one-dimensional manner, but are imbedded in a two-dimensional or three-dimensional basic flow which, in turn, depends on the waves via the boundary conditions. Concentration discontinuities (interfaces) are described by kinematic-shock theory. The kinematic shocks are shown to be horizontal, with the possible exception of discontinuities that separate the suspension from the sediment.

At downward-facing inclined walls conservation of mass enforces the existence of a boundary-layer flow with relatively large velocity. As $G/R^2 \to \infty$ and $G/R^4 \to 0$, where $G$ and $R$ are respectively a sedimentation Grashof number and a sedimentation Reynolds number, the entrainment of suspended particles into the boundary-layer flow of clear liquid is negligibly small. This provides an appropriate boundary condition for the basic flow of the suspension. Thus, in the double limit considered, a kinematic theory suffices to determine the convective flow of the suspension due to the presence of inclined walls.

As an example batch sedimentation in vessels with inclined plane or conical walls is investigated. The settling process is terminated after a time that can be considerably smaller than the time required in a vertical vessel under the same conditions. Depending on the initial particle concentration, there are centred kinematic waves that are linked to a continuous increase of the particle concentration in the suspension.

In an appendix, the flow in the boundary layer at a downward facing, inclined wall is investigated. With $G/R^2 \to \infty$ and $G/R^4 \to 0$ the boundary layer consists of an inviscid particle-free main part, a viscous sublayer at the wall, and a free shear sublayer at the liquid/particle interface.

## 1. Introduction

Kinematic waves are governed by continuity equations supplemented by functional relations between the fluxes and concentrations of the quantities under consideration (Whitham 1974). The theory of one-dimensional kinematic waves has been very successful in describing, among other things, the settling of particles in liquid-filled vertical vessels of constant cross-section (Wallis 1969, p. 190; Kluwick 1977). More recently, the theory of one-dimensional kinematic waves has been extended to deal with non-constant cross-section also (Baron & Wajc 1979; Anestis 1981).

Generalizations to more than one space co-ordinate are so far lacking. This may be partly because of the fact that in one-phase flow the generalization seems to be trivial, and the results not very interesting (Hayes 1974, p. 19). In two-phase flow, however, there are two coupled continuity equations to be satisfied, and further difficulties arise from the boundary conditions at inclined walls.

It has been known for about 60 years (Boycott 1920) that in the presence of inclined walls sedimentation rates can be several times larger than in vessels with vertical walls. Several models have already been proposed in order to provide a quantitative description of the phenomenon. The earlier models, which are reviewed by Hill, Rothfus & Li (1977) and Acrivos & Herbolzheimer (1979), were based on observations and did not rationally proceed from the basic equations of fluid mechanics. More recently, Hill *et al.* (1977) obtained numerical solutions of the two-phase flow equations for a very dilute suspension of particles that settle with a predetermined velocity relative to the fluid. Acrivos & Herbolzheimer (1979) developed an asymptotic theory in terms of a sedimentation Grashof number $G$ and a sedimentation Reynolds number $R$, with $G/R \to \infty$ and $G/R^4 \to \infty$. They indicated that the sedimentation rate can be predicted by the well-known Ponder–Nakamura–Kuroda formula (Ponder 1925; Nakamura & Kuroda 1937), and provided very interesting details of the flow field. The case $G/R \to \infty$, $G/R^4 = O(1)$ was also briefly discussed by Acrivos & Herbolzheimer (1979), but no solutions were given.

The present paper is concerned with the limit $G/R^2 \to \infty$ while $G/R^4 \to 0$. The analysis is based on the continuity equations for the particulate phase and the incompressible mixture, respectively, supplemented by a drift-flux relation describing the relative motion of the particles and the liquid in terms of the particle concentration. As the inertial terms are neglected in the bulk flow, the particle concentration is constant in planes perpendicular to the body force, i.e. in horizontal planes. It follows that there are horizontal kinematic-wave fronts (including one of two types of kinematic shocks) whose vertical motion depends on the two-dimensional or three-dimensional total volume flux. However, it is not concluded that the particle concentration is constant in the whole suspension. Thus, in contrast to that of Acrivos & Herbolzheimer (1979), the present theory also predicts sedimentation processes with centred waves which emerge from the bottom if the initial concentration is such that a simple concentration jump from the suspension to the sediment is not possible (i.e.

$$\alpha_a < \alpha_0 < \alpha_t,$$

cf. figure 3). Although the theory ignores interparticle forces that could be important in the high-concentration region near the bottom, centred waves have been observed in the one-dimensional flow in vessels with vertical walls, and good agreement has been found between the experimental results and the predictions according to kinematic-wave theory (Shannon *et al.* 1964; Shannon & Tory 1965).

At inclined, downward-facing walls the ordinary boundary conditions (tangential flow of both the liquid and the particulate phase) cannot be satisfied. This leads to a boundary layer in which the velocity is much larger than in the suspension. It turns out that the flow in the bulk of the suspension can be determined without any knowledge of the details of the flow in the boundary layer. The boundary layer, on the other hand, can be subdivided into an inviscid main part, a viscous sublayer at the wall, and a free shear layer at the interface between the clear liquid and the suspension.

The bulk flow's independence from the boundary-layer flow and the mainly inviscid boundary layer give rise to a flow field that is remarkably different from the limiting case $G/R^4 \to \infty$ as investigated by Acrivos & Herbolzheimer (1979).

## 2. Differential equations

Consider the unsteady flow of an incompressible mixture of a fluid (subscript 1) and solid particles of uniform shape and size (subscript 2). The volume fraction of particles (concentration) is $\alpha$, and the vectors of volume flux densities of fluid and particles are respectively $\mathbf{j}_1$ and $\mathbf{j}_2$. The following analysis is concerned with the bulk suspension away from the boundary layers at inclined walls. (The flow in the boundary layer is considered in the appendix. The flow in the clear liquid on top of the suspension is not considered, as under the present assumptions it does not effect the flow in the bulk suspension.) We anticipate that the volume-flux density (and velocity) of the liquid phase in the suspension is of the same order of magnitude as the terminal settling velocity $U$ of a single particle in the fluid at rest. This can be seen from the boundary condition at inclined walls (cf. §4), and is a result of the fact that the entrainment velocity into the boundary layers is of order $U$ (cf. appendix). Hence we introduce dimensionless variables by referring all volume flux densities and velocities to $U$, all lengths (including the spatial co-ordinates) to a characteristic length $H$ of the flow field, e.g. the height of the vessel, and the time $t$ to $H/U$.

With the total volume flux density $\mathbf{j} = \mathbf{j}_1 + \mathbf{j}_2$, the equations of continuity for the solid phase and the mixture are respectively

$$\frac{\partial \alpha}{\partial t} + \nabla . \mathbf{j}_2 = 0, \tag{1}$$

$$\nabla . \mathbf{j} = 0. \tag{2}$$

The pressure $p$ is referred to the hydrostatic pressure in the pure liquid (density $\rho_1$) by defining a dimensionless pressure $P$ according to

$$\nabla P = (\nabla p - \mathbf{g}\rho_1)/g\rho_1,$$

where $\mathbf{g}$ is the constant body force per unit mass (gravitational acceleration) and $g$ its absolute value.

Following the basic ideas of the one-dimensional theory of kinematic waves in two-phase systems (Wallis 1969, pp. 91 and 133) we are going to assume that the effects of inertia and viscosity are small. If $\rho_2 (> \rho_1)$ is the density of the particle material and $\nu_1$ is the kinematic viscosity of the liquid, which is assumed to be of the same order of magnitude as the kinematic viscosity of the suspension with the initial concentration $\alpha_0$, the buoyancy force, inertial forces and viscous forces are of the order of magnitude of $\alpha_0 g(\rho_2 - \rho_1)/\rho_1$, $U^2/H$ and $\nu_1 U/H^2$, respectively, with all forces referred to the unit mass of the liquid. Defining a sedimentation Grashof number $G$ and a sedimentation Reynolds number $R$ by

$$G = H^3 g\alpha_0(\rho_2 - \rho_1)/\rho_1 \nu_1^2, \quad R = HU/\nu_1, \tag{3}$$

we conclude that neglecting the viscosity of the suspension and inertial effects is justified if

$$G/R \to \infty, \quad G/R^2 \to \infty. \tag{4}$$

Both $G/R$ and $G/R^2$ are usually very large in applications of batch sedimentation. It follows that the momentum equation of the mixture is reduced to

$$\nabla P = \alpha(\rho_2/\rho_1 - 1)\,\mathbf{e}, \tag{5}$$

where $\mathbf{e}$ is the unit vector in the direction of gravity. Equation (5) indicates that the pressure is, in this approximation, equal to the hydrostatic pressure in the mixture. Furthermore, by the same reasoning as in the one-dimensional theory (Wallis 1969, p. 91), the momentum equation of the relative motion is reduced to a functional relation between the drift flux $\mathbf{j}_{21}$ and the concentration $\alpha$. With the drift flux defined by

$$\mathbf{j}_{21} = \mathbf{j}_2 - \alpha\mathbf{j} \tag{6}$$

the functional relation is written formally as

$$\mathbf{j}_{21} = f(\alpha)\,\mathbf{e}. \tag{7}$$

Equation (7) indicates that the drift-flux vector is parallel to the vector of the terminal settling velocity of a single particle in the quiescent fluid. The function $f(\alpha)$ is to be determined from suspension mechanics or by experiments. Often an empirical correlation of the power-law form

$$f(\alpha) = \alpha(1-\alpha)^n \quad (n = \text{const}) \tag{8}$$

is used. According to Richardson & Zaki (1954), cf. also Wallis (1969, p. 178), the value $n = 4\cdot65$ provides good results for small particle Reynolds numbers and very small ratios of particle diameter and vessel width. For larger particle Reynolds numbers smaller values of $n$ are appropriate. The correlation is terminated at a certain value $\alpha_s$ which is the particle concentration in the sediment (packed bed). For hard spheres $\alpha_s$ is known to be about 0·6.

Applying the curl operator to (5), we obtain

$$\nabla\alpha \times \mathbf{e} = 0. \tag{9}$$

Thus the concentration gradient must either vanish or be parallel to the gravity vector, i.e. the particle concentration in the suspension is constant in any horizontal plane at any instant of time.

We now introduce a space co-ordinate $z$ in the direction of $\mathbf{g}$. The co-ordinate surfaces $z = \text{const}$ are horizontal planes. The other two space co-ordinates can be chosen at our convenience. It then follows from (9) that

$$\alpha = \alpha(z,t). \tag{10}$$

The particle continuity equation (1) can now be essentially simplified. Introducing the drift-flux relation by means of (6) and (7) and satisfying the continuity equation (2) of the mixture, we obtain

$$\frac{\partial\alpha}{\partial t} + [\mathbf{j} + \mathbf{e}f'(\alpha)]\,.\,\nabla\alpha = 0, \tag{11}$$

where $f'(\alpha) = df/d\alpha$. Since $\mathbf{e}$ is in the direction of $z$ and $\alpha = \alpha(z,t)$, (11) can be rewritten as

$$\frac{\partial\alpha}{\partial t} + [j_z + f'(\alpha)]\frac{\partial\alpha}{\partial z} = 0, \tag{12}$$

where $j_z$ is the $z$-component of the total volume-flux vector $\mathbf{j}$. Equation (12) is of the same form as in the one-dimensional flow with constant cross-section. It describes the propagation of kinematic waves with the wave velocity

$$w = j_z + f'(\alpha). \tag{13}$$

In the one-dimensional flow in a vessel with vertical walls and constant cross-section, the total volume flux $j$ is constant. The constant is zero if there is a fixed bottom, which is usually the case with batch sedimentation. In a vessel with inclined walls, however, the flow is two-dimensional or three-dimensional, and $\mathbf{j}$ is to be determined from the continuity equation (2), supplemented by appropriate boundary conditions and the auxiliary condition (10). Thus the kinematic waves, which propagate in a quasi-one-dimensional manner, are imbedded in a two-dimensional or three-dimensional total flow field which, in turn, depends on the waves via the boundary conditions (cf. §4).

Differentiating the kinematic-wave equation (12) with respect to any co-ordinate $x$ orthogonal to the $z$-axis and taking into account that, according to (10), $\alpha$ does not depend on $x$, we obtain

$$\frac{\partial j_z}{\partial x}\frac{\partial \alpha}{\partial z} = 0. \tag{14}$$

This condition is satisfied if $\partial j_z/\partial x = 0$ or if $\partial \alpha/\partial z = 0$. In the latter case it follows from (12) that $\alpha = \text{const}$, and (12) is satisfied trivially. The former case, however, yields

$$j_z = j_z(z,t). \tag{15}$$

This is an auxiliary condition which has to be obeyed when seeking for solutions of the continuity equation (2). The special case $\alpha = \bar{\alpha} = \text{const}$ seems to be an exception. In this case, however, a solution that is stable with respect to small perturbations of the constant concentration is being sought. Thus, if $\alpha = \bar{\alpha} + \epsilon\alpha'(z,t)$ with $\epsilon \to 0$ it is required that $j_z = \bar{j}_z + \epsilon j_z'$. Taking into account that $\partial\bar{\alpha}/\partial z = 0$ but $\partial\alpha'/\partial z \neq 0$ we obtain from (14) $\partial\bar{j}_z/\partial z = 0$. Therefore, the condition (15) is also applied to the case of constant concentration.

For steady flow, e.g. for a continuous thickening process, (12) yields $\alpha = \text{const}$ unless $j_z = -f'(\alpha)$ or a discontinuity appears. We shall not, however, proceed further with steady-flow problems in this paper.

For unsteady flow, the wave fronts $\zeta(t,z) = \text{const}$ are introduced. The co-ordinates $(t, z, \ldots)$ are replaced by the new independent variables $(\tau, \zeta, \ldots)$ with

$$t = \tau, \quad \frac{\partial z}{\partial \tau} = j_z + f'(\alpha). \tag{16a, b}$$

This transforms the kinematic-wave equation (12) into $\partial\alpha/\partial\tau = 0$, with the general solution

$$\alpha = \alpha(\zeta). \tag{17}$$

Thus, as in one-dimensional flow with constant cross-section, the particle concentration remains constant on wave fronts. The function $\alpha(\zeta)$ is to be determined from initial conditions together with boundary conditions and – perhaps – jump conditions at discontinuities (kinematic shocks).

It might be tempting to conclude from (17) that in the case of a constant initial concentration the concentration in the suspension remains constant at all times. Although, in fact, this may happen under certain circumstances (cf. the examples in

§§5.1 and 5.4) the conclusion is not true in general. For the initial conditions may be such that centred kinematic waves appear which give rise to a continuous variation of the particle concentration in the suspension (cf. the examples in §§5.2 and 5.3).

## 3. Kinematic-shock relations

Discontinuities in the concentration $\alpha$ propagate as kinematic-shock waves. Such discontinuities separate the suspension from the clear fluid on top and from the sediment at the bottom of the vessel, and under certain conditions they may also appear within the suspension.

We shall denote quantities immediately behind the kinematic shock wave by ^, while quantities without the circumflex refer to the state immediately in front of the shock. In the shock the particle volume fraction jumps from $\alpha$ to $\hat{\alpha}$. Since inertial terms, i.e. convective momentum flux, and friction are neglected, the conservation of momentum flux across the shock implies that the pressure has to be the same on both sides of the shock. Thus $\hat{p} = p$ in any point of the shock surface. If $\mathbf{t}$ is a vector within the tangential plane in any point of the shock surface, it follows that the inner derivative of the pressure $\mathbf{t}.\nabla p$ has to be the same on both sides of the surface. Substituting according to (5) and taking into account the fact that $\alpha$ is different on both sides of the discontinuity, we obtain $\mathbf{t}.\mathbf{e} = 0$. This shows that the kinematic shock surface is horizontal provided that (5) is satisfied on both sides of the shock. This is not necessarily the case in the sediment layer in which the particles support each other.

The propagation velocity $W$ of the kinematic-shock waves can be determined in the same manner as in the well-known one-dimensional case (cf. Wallis 1969, p. 134). For a (possibly inclined) shock that separates the suspension with concentration $\alpha$ from the sediment, which is at rest and has the concentration $\alpha_s$, conservation of the volume of the solid phase yields

$$W = -\frac{f(\alpha)}{\alpha_s - \alpha}(\mathbf{e}.\mathbf{n}), \tag{18}$$

where $\mathbf{n}$ is the unit normal vector of the shock surface (i.e. sediment surface).

For a horizontal kinematic shock the normal component of the total volume flux is conserved if

$$\hat{j}_z = j_z, \tag{19}$$

and from the conservation of particulate volume one obtains

$$W = j_z + \frac{f(\hat{\alpha}) - f(\alpha)}{\hat{\alpha} - \alpha}. \tag{20}$$

A horizontal shock remains horizontal only if $W = W(z,t)$. Together with (10) this again yields (15).

## 4. Boundary conditions at walls

An ordinary boundary condition would require that the flow of both the liquid phase and the solid phase (particle cloud) be tangential at a wall. At downward-facing inclined walls, however, that condition cannot be satisfied within the framework of the kinematic model, since, according to (7), the drift flux is always in the vertical direction. This is also the reason why our basic equation (12) is of the same form as if the cross-section were constant. It therefore contradicts the continuity equation of one-dimensional flow with variable cross-section $A$. The conclusion is that the theory of kinematic waves fails near downward-facing inclined walls. Owing to the vertical drift flux, there is a thin layer of clear liquid at the downward-facing inclined wall. This has already been observed in all relevant experimental investigations (see e.g. Hill *et al.* 1977; Acrivos & Herbolzheimer 1979). The volume flux in the boundary layer has to compensate for the deficiency of (12), which is a simplified continuity equation for the particle phase. Thus the velocity in the boundary layer is much larger than in the bulk of the suspension. Inertial effects and/or viscosity can no longer be ignored in this layer but are essential for balancing the buoyancy forces, which are due to the difference between the particle concentration in the boundary layer and that in the bulk of the suspension.

The thickness $\delta$ of, and the tangential velocity $u$ in, the boundary layer can be easily estimated. Since $\delta$ is referred to $H$, and $u$ is referred to $U$, continuity of volume flux requires $\delta u$ to be of order unity. Furthermore, the inertial terms (which have been neglected so far in the momentum equations) are of the same order of magnitude as the buoyancy term (which has been retained) if $u^2$ is as large as $G/R^2$; cf. (3)–(5). Similarly, the viscous terms are of the order of the buoyancy term if $u^3$ is as large as $G/R$. Thus inertial effects and viscosity are both of importance in the boundary layer if $G^{\frac{1}{2}}R^{-1}$ and $G^{\frac{1}{3}}R^{-\frac{1}{3}}$ are of the same order of magnitude, i.e. if $G/R^4 = O(1)$. Viscosity dominates the flow in the boundary layer of clear liquid if $G/R^4 \to \infty$. It is this case that has been investigated in detail by Acrivos & Herbolzheimer (1979). On the other hand, if $G/R^4 \to 0$ viscous effects are either small or confined to very thin sublayers of the boundary layer, which is mainly inviscid and occupies a thickness $\delta = O(G^{-\frac{1}{2}}R)$. The latter case will be studied in what follows. Note that $G/R^4 \to 0$ together with $G/R^2 \to \infty$ implies $R \to \infty$.

There are no unbalanced buoyancy forces in the suspension as long as (10) is satisfied. As, furthermore, viscous shear stresses are negligibly small in the boundary layer, the entrainment of suspended particles into the boundary-layer flow of clear liquid is negligibly small, too. (For a more detailed analysis see the appendix.) On the other hand, the boundary layer can be maintained particle-free only if the normal component of the particle volume flux in the suspension $j_{2n}$ vanishes at the wall. With (6) and (7) we immediately obtain the boundary condition

$$\alpha j_n + f(\alpha) \cos\theta = 0 \quad \text{at the wall,} \tag{21}$$

where $j_n$ is the normal component of the total volume flux $\mathbf{j}$ and $\theta$ is the angle between the (vertical) $z$-axis and the wall normal pointing into the suspension (figure 1). Since $0 < \theta < \frac{1}{2}\pi$ it follows from (21) that $j_n < 0$, i.e. the total volume flux in the suspension is always towards the wall.

## 5. Examples: batch sedimentation in vessels with inclined plane or conical walls

We shall now study simple examples of two-dimensional or axisymmetric flow. For a two-dimensional flow in a Cartesian $(x, z)$-plane the vessel consists of a horizontal bottom, two plane side walls with inclination angle $\theta$, either roof-like (inclined toward each other, figure 2$a$) or parallel to each other (figure 2$b$), and two vertical side walls parallel to the $(x, z)$-plane. In the axisymmetric case the vessel is a truncated, circular

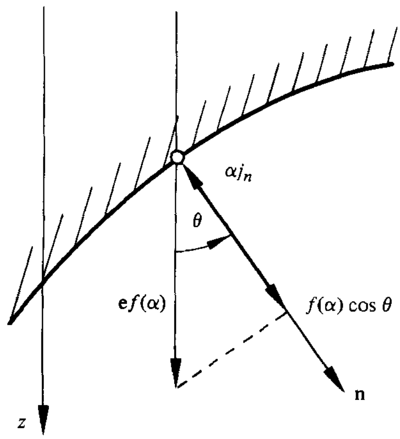


FIGURE 1. Boundary condition at downward-facing inclined wall.

cone with vertical axis and horizontal bottom (figure 2*a*). In this case $x$ is the radial co-ordinate. The top surface is always supposed to be horizontal and may either be a solid wall or a free surface of the fluid. The reference length $H$ for the dimensionless variables is defined as shown in figures 2(*a*, *b*).

The present theory applies only if the boundary-layer thickness $\delta$ is much smaller than the width of the vessel, i.e. $\delta/h \cot\theta = o(1)$ and $\delta/a \sin\theta = o(1)$, respectively. With the orders of magnitude given in §4 the conditions are respectively

$$1/h\cot\theta = o(G^{\frac{1}{2}}R^{-1}) \quad \text{and} \quad 1/a\sin\theta = o(G^{\frac{1}{2}}R^{-1}).$$

Very narrow vessels (widths comparable to the boundary-layer thickness) have recently been studied by Herbolzheimer & Acrivos (1981).

The continuity equation (2) of the mixture can be rewritten as

$$\frac{1}{x^\sigma}\frac{\partial(x^\sigma j_x)}{\partial x}+\frac{\partial j_z}{\partial z}=0, \tag{22}$$

where $\sigma = 0$ for two-dimensional flow, $\sigma = 1$ for axisymmetric flow, and $j_x$, $j_z$ are the $x$-, $z$-components of the total volume-flux density $\mathbf{j}$. Taking (15) into account, (22) can be integrated at once to yield

$$j_x = -\frac{x}{1+\sigma}\frac{\partial j_z}{\partial z}+C(z,t)\cot\theta, \tag{23}$$

with an arbitrary function $C(z,t)$. In case of roof-shaped or conical walls, symmetry with respect to $x = 0$ requires

$$C(z,t) \equiv 0. \tag{24a}$$

For parallel walls, however, $C(z,t)$ is to be determined from the boundary condition at the upward-facing inclined wall. It states that the normal flux component

$$j_n = j_z\cos\theta - j_x\sin\theta$$

vanishes at the surface of the sediment layer with height $s$, i.e. at $(x+a)\tan\theta = z+s$. This yields

$$C(z,t) = j_z+(z+s-a')\frac{\partial j_z}{\partial z}, \tag{24b}$$

where $a' = a\tan\theta$.

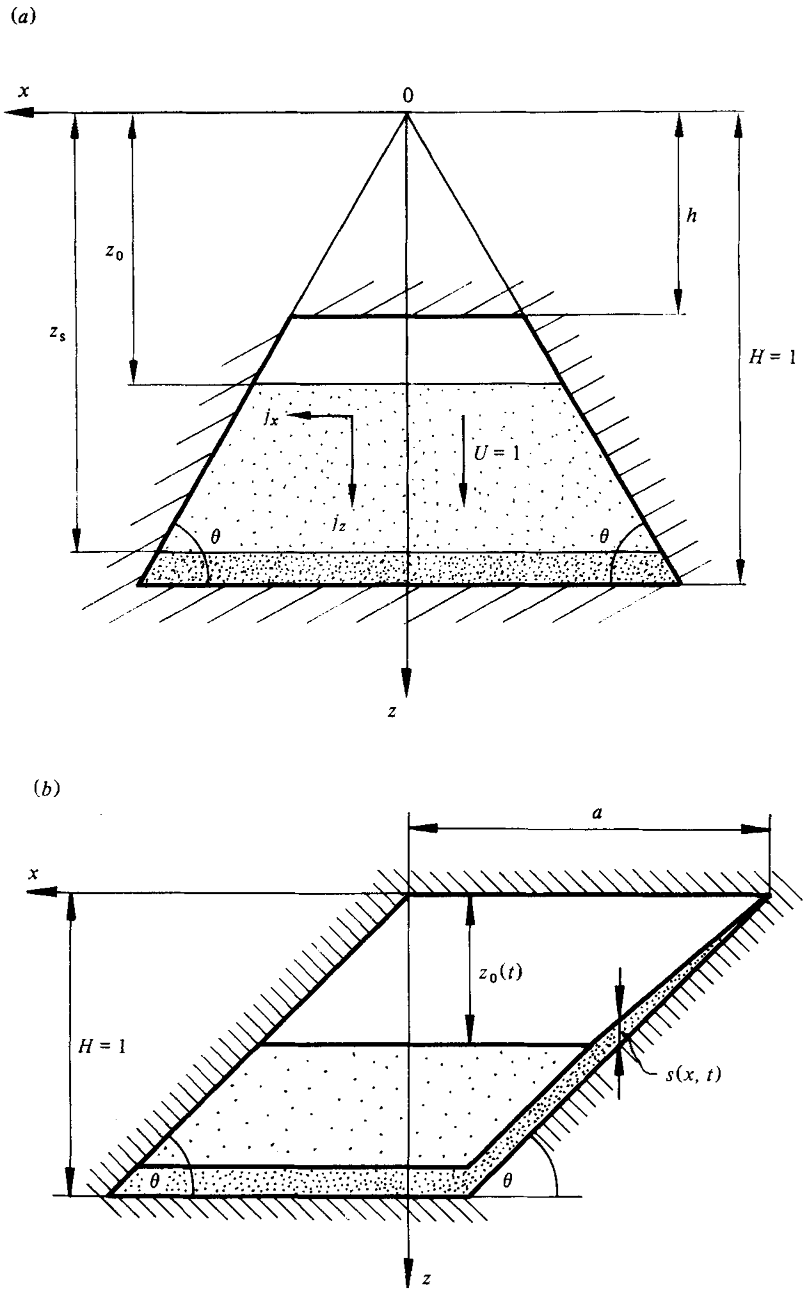


FIGURE 2. Batch sedimentation in vessels with inclined plane or conical walls: (a) roof-shaped plane walls or conical wall; (b) parallel plane walls.

At the downward-facing inclined wall $x = z\cot\theta$ the normal flux component $j_n = j_z\cos\theta - j_x\sin\theta$ has to satisfy the boundary condition (21). Substituting for $j_x$ according to (23), we obtain

$$\frac{z}{1+\sigma}\frac{\partial j_z}{\partial z} + j_z = -\frac{f(\alpha)}{\alpha} + C(z,t). \tag{25}$$

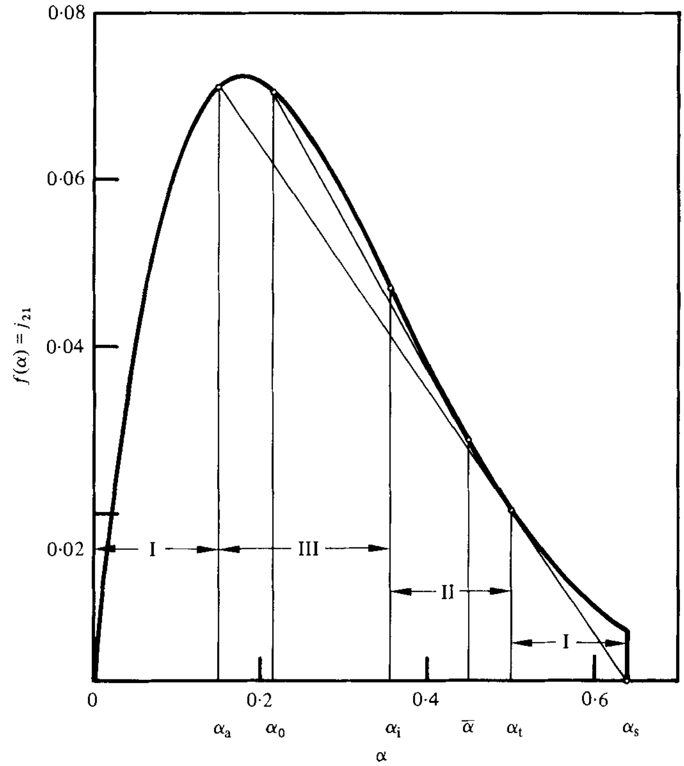


FIGURE 3. Types of sedimentation depending on the initial concentration $\alpha_0$. Drift-flux relation according to (8), $n = 4{\cdot}6$; $\alpha_s = 0{\cdot}64$, $\alpha_t = 0{\cdot}502$, $\alpha_i = 0{\cdot}357$, $\alpha_a = 0{\cdot}151$.

Equation (25) and the kinematic-wave equation (12) comprise a system of two first-order partial differential equations for the two unknowns $\alpha(z,t)$ and $j_z(z,t)$. The coupling of the equations is due to the boundary-layer flow at the inclined walls, and has no counterpart in the well-known one-dimensional theory of vessels with vertical walls.

An interesting consequence of (25) and (23) is that an initial condition for the total flux $\mathbf{j}$ cannot be prescribed independently of the initial particle concentration $\alpha_0$. Rather $j_z$ at initial time $t = 0$ is to be determined by integrating (25) with $\alpha = \alpha_0$, and $j_x$ at $t = 0$ follows from (23). The reason for this peculiar restriction is in the failure of the kinematic-wave theory to describe properly the starting-up process, which is controlled by dynamic effects.

Depending on the initial concentration $\alpha_0$, three different types of sedimentation come into operation (figure 3). The concentrations $\alpha_i$, $\alpha_t$ and $\alpha_a$ that separate the various sedimentation types from each other are respectively the concentrations at the inflection point of the drift-flux curve, at the point where a straight line through the sediment point $\alpha_s$ is tangent to the drift-flux curve, and at the point where the tangent crosses the curve. Thus $\alpha_i$, $\alpha_t$ and $\alpha_a$ are to be determined from

$$f''(\alpha_i) = 0, \quad f(\alpha_a)/(\alpha_a - \alpha_s) = f(\alpha_t)/(\alpha_t - \alpha_s) = f'(\alpha_t). \tag{26}$$

The classification is exactly the same as in the well-known one-dimensional theory of a vessel with vertical walls (cf. Wallis 1969, pp. 191–194). For this classification is based on the relative magnitude of the kinematic-wave velocities and kinematic-shock velocities, and is independent of the total flux **j**.

### 5.1. *Roof-shaped and conical walls, sedimentation type I* ($\alpha_0 \leqslant \alpha_a$ *or* $\alpha_0 \geqslant \alpha_t$)

A kinematic shock separating the suspension with initial concentration $\alpha_0$ from the sediment with concentration $\alpha_s$ is possible. This shock moves, according to (20), with the constant dimensionless velocity $W = -f(\alpha_0)/(\alpha_s - \alpha_0)$. Since at $t = 0$ the sedimentation process starts with no sediment at the bottom ($z = 1$) we obtain the following position of the shock separating the sediment from the suspension:

$$z_s = 1 - \frac{f(\alpha_0)}{\alpha_s - \alpha_0}t. \tag{27}$$

In the suspension the concentration remains constant and equal to $\alpha_0$. Thus the kinematic-wave equation (12) is trivially satisfied in this case, and from integrating (25) with $C(z, t) \equiv 0$ we obtain

$$j_z = \frac{f(\alpha_0)}{\alpha_0}\left[\left(\frac{z_s}{z}\right)^{1+\sigma} - 1\right]. \tag{28}$$

Here, a function of integration has already been determined such that $j_z = 0$ at $z = z_s(t)$, i.e. at the sediment, which is at rest.

As $z \rightarrow 0$ the flux density $j_z$ increases beyond bounds. Thus inertial effects can no longer be ignored and one of the basic assumptions of kinematic wave theory is violated at and near the tip of the vessel.

Equation (28), which is valid in the suspension, shows that $j_z$ is positive, i.e. directed downwards. This results in an enhanced velocity of the kinematic shock separating the suspension from the clear liquid on top. With $W = dz_0/dt$ a differential equation of the shock position $z = z_0(t)$ is obtained from the kinematic-shock relation (20). Substituting according to (28) and integrating, we obtain

$$z_0^{2+\sigma} - h^{2+\sigma} = \frac{\alpha_s - \alpha_0}{\alpha_0}\left\{1 - \left[1 - \frac{f(\alpha_0)}{\alpha_s - \alpha_0}t\right]^{2+\sigma}\right\}. \tag{29}$$

By a suitable choice of a constant of integration, (29) has been made to satisfy the initial condition $z_0 = h$ at $t = 0$ (cf. figure 2*a*). According to (29) the path of the kinematic shock separating the suspension from the clear fluid is a quadratic (two-dimensional case, $\sigma = 0$) or cubic (axisymmetric case, $\sigma = 1$) parabola in the $(z, t)$-plane (figure 4).

The settling process is terminated after a certain time $t_s$. It can be determined either from the intersection of the upper and lower shock paths (figure 4), or from equalizing the total volume of the solid phase both in the sediment and in the initial suspension. The result is

$$t_s = \frac{\alpha_s - \alpha_0}{f(\alpha_0)}\left\{1 - \left[1 - (1 - h^{2+\sigma})\frac{\alpha_0}{\alpha_s}\right]^{1/(2+\sigma)}\right\}. \tag{30a}$$

The limiting case of a very dilute suspension, i.e. $\alpha_0 \rightarrow 0$, is of particular interest. With $f(\alpha_0) \rightarrow \alpha_0$ as $\alpha_0 \rightarrow 0$, cf. (8), it follows from (30*a*) that the sedimentation time is

$$t_s = \frac{1}{2 + \sigma}(1 - h^{2+\sigma}) \quad \text{as} \quad \alpha_0 \rightarrow 0. \tag{30b}$$

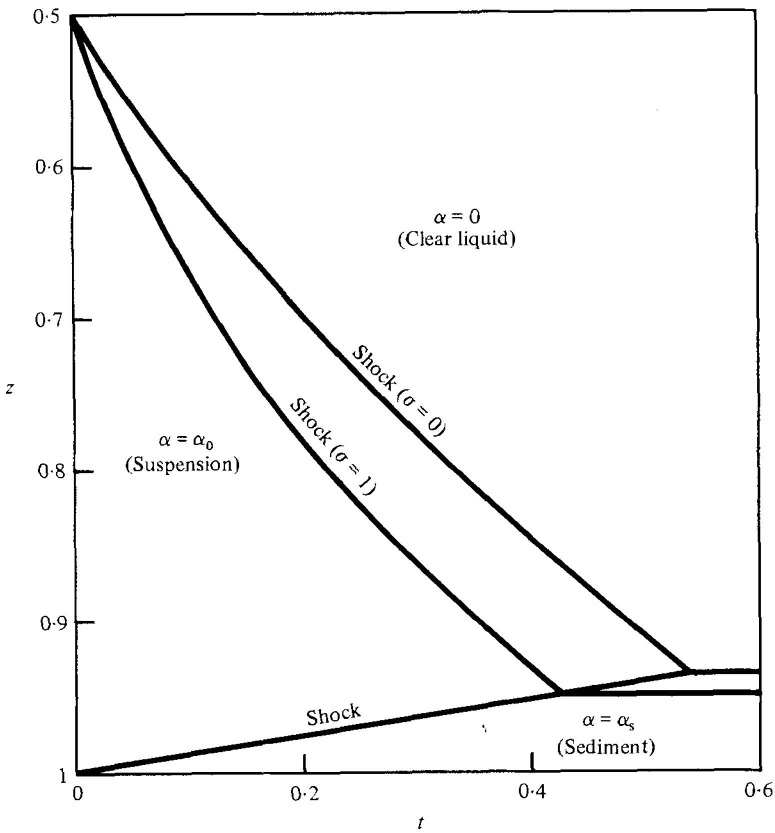


FIGURE 4. Type I sedimentation in a vessel with roof-shaped plane ($\sigma = 0$) or conical ($\sigma = 1$) walls; $h = 0{\cdot}5$, $n = 4{\cdot}6$, $\alpha_0 = 0{\cdot}106$, $\alpha_s = 0{\cdot}64$.

This is the same result as obtained from the PNK theory (Ponder 1925; Nakamura & Kuroda 1937), which, however, does not give any details of the flow field. If the convective flow were neglected the sedimentation time in the limiting case $\alpha_0 \rightarrow 0$ would simply be that of a single particle in a fluid at rest, i.e. $t_s = 1-h$. This is as much as three times larger than that given by (30*b*).

Experiments with very dilute suspensions in conical vessels were performed by Hill *et al.* (1977). Since the sedimentation Reynolds number was not very large and, besides, the vessels were filled to the tip, where kinematic-wave theory does not apply (cf. (28)), the experiments of Hill *et al.* (1977) cannot be compared with the present theory.

Let us now return to the more general case of finite particle concentration. Since $\alpha = \alpha_0 = \text{const}$ it is easy to determine the instantaneous streamlines $\psi(z, x) = \text{const}$ of both the liquid (subscript 1) and the solid phase (particle cloud, subscript 2). The stream functions $\psi_1$ and $\psi_2$ are defined by

$$\frac{\partial \psi_{1,2}}{\partial x} = x^{\sigma} j_{1,2z}, \quad \frac{\partial \psi_{1,2}}{\partial z} = -x^{\sigma} j_{1,2x}. \tag{31}$$

Now $\mathbf{j}_2$ with components $j_{2z}, j_{2x}$ is related to $\alpha$ and $\mathbf{j}$ with components $j_z, j_x$ according to

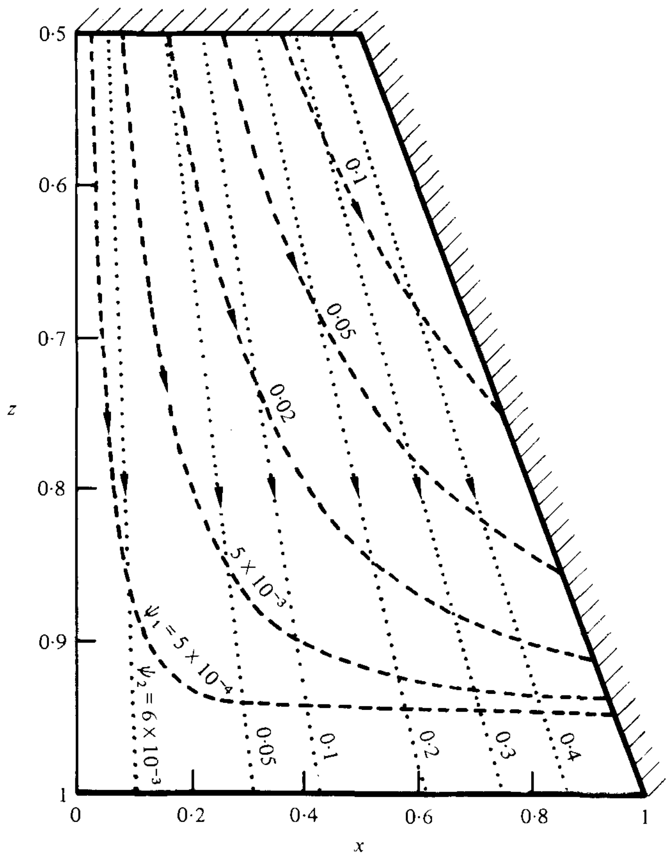


FIGURE 5. Instantaneous streamlines of liquid (– – – –) and solid (......) phases at initial time $t = 0$ (particle streamlines and particle paths are identical). Vessel: truncated cone; $h = 0{\cdot}5$, $n = 4{\cdot}6$. Initial concentration ($\alpha_0 = 0{\cdot}106$) of type I (no centred wave).

(6) and (7), and $\mathbf{j}_1$ follows from $\mathbf{j}_1 = \mathbf{j} - \mathbf{j}_2$. Using the results (28) and (23) and integrating (31), we obtain

$$\psi_1 = \frac{x^{1+\sigma}}{1+\sigma}\frac{f(\alpha_0)}{\alpha_0}\left[(1-\alpha_0)\left(\frac{z_s}{z}\right)^{1+\sigma} - 1\right], \tag{32a}$$

$$\psi_2 = \frac{x^{1+\sigma}}{1+\sigma} f(\alpha_0)\left(\frac{z_s}{z}\right)^{1+\sigma}. \tag{32b}$$

Thus the instantaneous streamlines of the solid phase are straight lines $x = Kz$, with $K$ depending on the parameter $t$ since $z_s = z_s(t)$. Therefore the particle paths, too, are straight lines originating from the intersection of the inclined walls (i.e. the cone tip in the axisymmetric case). The liquid streamlines in the suspension region are bent towards the inclined walls and, in contrast to the case of vertical walls, are directed downwards (figure 5).

### 5.2. *Roof-shaped and conical walls, sedimentation type II* ($\alpha_i \leqslant \alpha_0 < \alpha_t$)

A kinematic shock between $\alpha_0$ and $\alpha_s$ is not possible since it would move with lower speed than the kinematic waves in front of it. Thus there is a kinematic shock with a

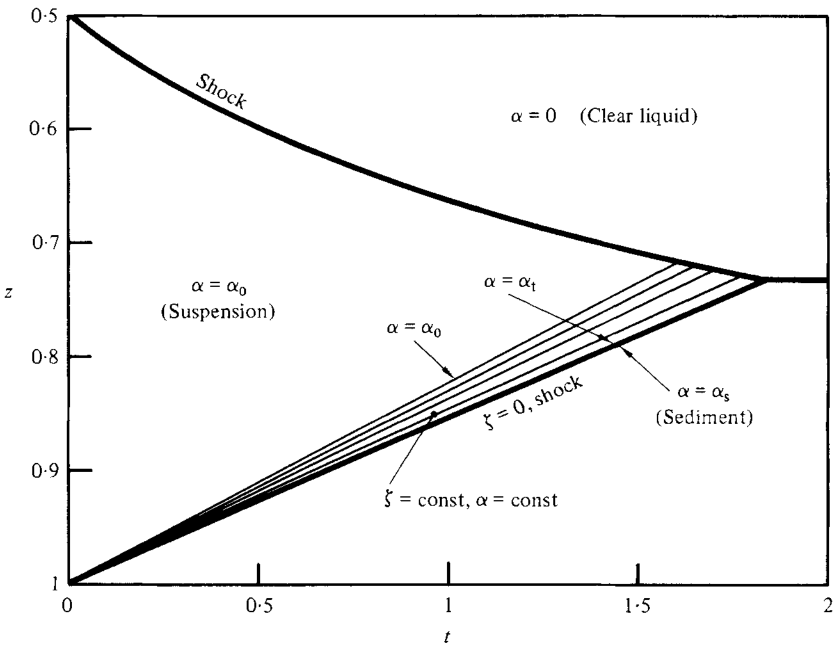


FIGURE 6. Type II sedimentation in a truncated cone; $h = 0{\cdot}5$, $n = 4{\cdot}6$, $\alpha_0 = 0{\cdot}45$, $\alpha_t = 0{\cdot}502$, $\alpha_s = 0{\cdot}64$.

concentration jump from $\alpha_t$ to $\alpha_s$, but the increase in concentration from $\alpha_0$ to $\alpha_t$ is continuous and can be described by centred kinematic waves (figure 6).

In order to determine the centred waves it is convenient to introduce the wave variable $\zeta$ as a new independent variable defined by (16*a*, *b*). By this transformation (25) with $C(z,t) \equiv 0$ becomes

$$\frac{z}{1+\sigma}\frac{\partial j_z}{\partial \zeta} + \left[j_z + \frac{f(\alpha)}{\alpha}\right]\frac{\partial z}{\partial \zeta} = 0. \tag{33}$$

Equations (33) and (16*b*) are a system of two equations for the two unknowns $j_z(\zeta,\tau)$ and $z(\zeta,\tau)$. According to (17) $\alpha = \alpha(\zeta)$, with $\alpha(\zeta)$ to be determined from initial and boundary conditions. Since in a centred wave all waves have their origin in the same point, $\alpha(\zeta)$ can be chosen arbitrarily in this region. The simplest choice is the linear relation

$$\alpha = \alpha_t - \zeta, \tag{34}$$

which satisfies the boundary conditions $\alpha = \alpha_t$ at the shock front $\zeta = 0$, and $\alpha = \alpha_0$ at the wave $\zeta = \alpha_t - \alpha_0$ separating the centred-wave region from the region of constant concentration. Further boundary and initial conditions are

$$j_z = 0 \quad (\zeta = 0,\ \tau > 0), \tag{35a}$$

$$z = 1 \quad (\tau = 0,\ 0 \leqslant \zeta \leqslant \alpha_t - \alpha_0). \tag{35b}$$

Equation (35*a*) is due to the fact that the total volume flux is continuous across the kinematic shock with the sediment behind it being at rest. Equation (35*b*) indicates that the wave centre is at the bottom.

The system of equations (33) and (16*b*) is in the form of compatibility conditions, and may be solved by a method of characteristics. Solutions in closed form can be obtained by the method of strained co-ordinates based on the assumption that $\alpha_t - \alpha_i$ is very small compared to unity. This is quite well satisfied by the usual drift-flux correlations (cf. figure 3). Thus we expand in terms of $\zeta$ as follows:

$$z = z_s(\tau) + \zeta z^*(\tau) + \ldots, \tag{36a}$$

$$j_z = \zeta j_z^*(\tau) + \ldots. \tag{36b}$$

In (36*b*) the first-order term has been omitted in order to satisfy the boundary condition (35*a*). Introducing the expansions (36*a, b*) into (16*b*) and (33) and solving the perturbation equations subject to the boundary condition (35*b*), we finally obtain (with $\tau = t$)

$$z_s = 1 + f'(\alpha_t)\, t, \tag{37}$$

$$z^* = \frac{f''(\alpha_t)}{m f'(\alpha_t)} z_s (1 - z_s^m) \quad (m \neq 0), \tag{38a}$$

$$j_z^* = \frac{m+1}{m} f''(\alpha_t)(1 - z_s^m) \quad (m \neq 0), \tag{38b}$$

$$z^* = -\frac{f''(\alpha_t)}{f'(\alpha_t)} z_s \ln z_s \quad (m = 0), \tag{39a}$$

$$j_z^* = -f''(\alpha_t) \ln z_s \quad (m = 0), \tag{39b}$$

$$m = -\left[1 + \frac{(1+\sigma) f(\alpha_t)}{\alpha_t f'(\alpha_t)}\right]. \tag{40}$$

This is the solution in the centred-wave region. Unlike the one-dimensional flow in vessels with vertical walls, the wave fronts are not straight lines any more. Note that $f''(\alpha_t)$ is of order $\alpha_t - \alpha_i$, since $f''(\alpha_i) = 0$. Thus in the centred-wave region, the total flux $j_z$ is of order $(\alpha_t - \alpha_i)^2$.

For the region of constant concentration, which is above the centred-wave region, we have to solve (25) with $\alpha = \alpha_0$. It is required that the solution be continuous at the limiting wave front $\zeta = \alpha_t - \alpha_0$. Thus the boundary condition is

$$j_z = (\alpha_t - \alpha_0) j_z^*(t) \quad \text{at} \quad z = z_s(t) + (\alpha_t - \alpha_0) z^*(t). \tag{41}$$

The solution in the region $\alpha = \alpha_0$ is

$$j_z = \frac{f(\alpha_0)}{\alpha_0}\left[\left(\frac{z_s}{z}\right)^{1+\sigma} - 1\right] + (\alpha_t - \alpha_0)\frac{N}{m}(1 - z_s^m)\left(\frac{z_s}{z}\right)^{1+\sigma} + \ldots \quad (m \neq 0), \tag{42}$$

with $z_s$ according to (37), and

$$N = \left[m + 1 + \frac{(1+\sigma) f(\alpha_0)}{\alpha_0 f'(\alpha_t)}\right] f''(\alpha_t). \tag{43}$$

The solution for $m = 0$ can be obtained from (42) by applying the limit process $m \to 0$.

In a first approximation, with terms of order $(\alpha_t - \alpha_i)^2$ being neglected, the solution (42) agrees formally with the solution (28) describing sedimentation of type I. Only the function $z_s(t)$ is somewhat different in both cases (cf. (27) and (37)). Therefore the position $z_0(t)$ of the kinematic shock separating the suspension from the clear liquid on

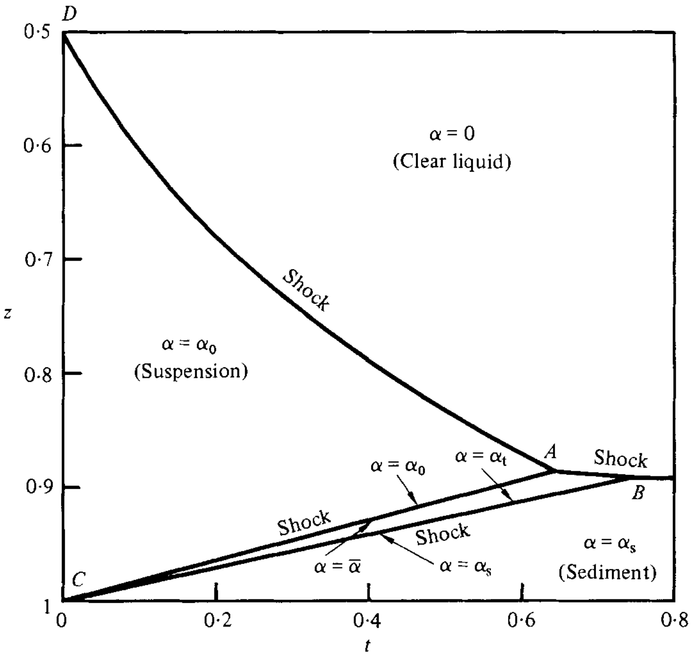


FIGURE 7. Type III sedimentation in a truncated cone; $h = 0{\cdot}5$, $n = 4{\cdot}6$, $\alpha_0 = 0{\cdot}217$, $\bar{\alpha} = 0{\cdot}45$, $\alpha_t = 0{\cdot}502$, $\alpha_s = 0{\cdot}64$.

top also corresponds – in a first approximation – to that of type I, (29). The result is

$$z_0^{2+\sigma} - h^{2+\sigma} = \frac{f(\alpha_0)}{\alpha_0 f'(\alpha_t)}\{[1+f'(\alpha_t)\,t]^{2+\sigma} - 1\} + \dots, \tag{44}$$

where the neglected terms are of order $(\alpha_t - \alpha_i)^2$.

Finally, by comparing the total volume of the solid phase in the sediment with that in the initial suspension we obtain the sedimentation time

$$t_s = -\frac{1}{f'(\alpha_t)}\left\{1 - \left[1 - (1-h^{2+\sigma})\frac{\alpha_0}{\alpha_s}\right]^{1/(2+\sigma)}\right\}. \tag{45}$$

This result is analogous to (30*a*).

### 5.3. *Roof-shaped and conical walls, sedimentation type III* ($\alpha_a < \alpha_0 < \alpha_i$)

A continuous connection between the centred wave and the region of constant initial concentration is not possible. Rather there is a third kinematic shock which separates the two continuous regions of the suspension (figure 7). The concentration $\bar{\alpha}$ immediately behind this shock is determined solely by the drift-flux relation. It is given by the point where a straight line through the point of the initial state ($\alpha = \alpha_0$) is tangent to the drift-flux curve (figure 3). Thus the shock speed is the same as the wave velocity immediately behind the shock, and the shock path $CA$ in the $(z, t)$-plane (figure 7) coincides with the limiting wave front ($\alpha = \bar{\alpha}$) of the centred waves. The centred waves can be determined from the equations derived in the §5.2, i.e. (34) and (36)–(40).

Furthermore, the shock path $CB$ is a straight line, and is again given by (37). With respect to the sedimentation time this implies that (45) also applies to type III.

On the same arguments as for type II, the total flux $j_z$ is small and of higher order in the centred-wave region, while in the constant-concentration region it is, to a first approximation, given by (28) with $z_s(t)$ evaluated according to (37). It follows that the liquid–suspension interface is again given approximately by (44) until, at a point $A$ (figure 7), it meets the kinematic shock that is the upper boundary of the centred-wave region. For larger times ($t > t_A$) the interface is influenced by the centred waves. With $j_z$ negligible in this region, and $\alpha$ approximated by $\alpha_t$, (20) yields the kinematic-shock velocity $W = f(\alpha_t)/\alpha_t + \ldots$. This is a constant, and section $AB$ of the interface is approximately a straight line (figure 7).

### 5.4. *Parallel plane walls, sedimentation type I* ($\alpha_0 \leqslant \alpha_a$ *or* $\alpha_0 \geqslant \alpha_t$)

At the upward-facing inclined wall sediment can accumulate. We assume that the sediment remains at rest, which requires sufficiently small inclination angles, depending on particle shape and material. The assumption is superfluous for very small initial concentrations $\alpha_0 \ll 1$, since in this case the thickness of the sediment layer is negligible.

As a kinematic shock between the suspension with initial concentration $\alpha_0$ and the sediment with concentration $\alpha_s$ is possible if the value of $\alpha_0$ is in the regime of type I, the concentration remains constant in the suspension.† It then follows from the kinematic-shock relation (18) that the rate of increase of the sediment height $s$ (measured in the vertical direction, cf. figure 2$b$) due to particle settling is

$$f(\alpha_0)/(\alpha_s - \alpha_0) = \text{const.}$$

Note that the rate of increase is independent of the inclination angle $\theta$. It is therefore the same above the horizontal bottom and above the upward-facing inclined wall. Since no particles can settle from the clear liquid, the sediment height $s$ does not increase with time any more above the liquid–suspension interface, i.e. for $z < z_0(t)$, where $z_0(t)$ is still to be determined. Hence the sediment height becomes

$$s = At \quad (x' \geqq z_0(t) + At), \tag{46a}$$

$$s = A\tau(x') \quad (x' \leqq z_0(t) + At), \tag{46b}$$

with

$$A = f(\alpha_0)/(\alpha_s - \alpha_0), \tag{47}$$

$$x' = (x + a)\tan\theta, \tag{48}$$

and $\tau(x')$ to be determined from

$$x' = z_0(\tau) + A\tau. \tag{49}$$

Since $\alpha = \alpha_0 = \text{const}$, the total volume flux in the suspension can easily be obtained by integrating (25) with $C(z, t)$ substituted according to (24$b$). A function of integration is determined from the condition that the vertical flux component $j_z$ has to vanish at the horizontal suspension–sediment interface above the bottom, i.e. at

$$z = 1 - s = 1 - At.$$

† In the presence of an upward-facing inclined wall the rather large initial concentrations in the regimes II and III seem to give rise to some additional problems that are beyond the scope of the present analysis.

This yields

$$j_z = \frac{f(\alpha_0)}{\alpha_0}\frac{1-z-At}{a'-At}, \qquad (50)$$

where, as before, $a' = a\tan\theta$ has been introduced. Furthermore, from (23) the horizontal flux component

$$j_x = \frac{f(\alpha_0)}{\alpha_0}\frac{1+x'-2(z+At)}{(a'-At)\tan\theta} \qquad (51)$$

is obtained.

The position of the liquid–suspension interface $z = z_0(t)$ can now be determined from the kinematic-shock relation (20) with $W = dz_0/dt$. Performing the integration yields

$$z_0(t) = \left(1+\frac{\alpha_s a'}{\alpha_s - 2\alpha_0}\right)[1-(1-At/a')^{(\alpha_s-\alpha_0)/\alpha_0}] - \frac{2(\alpha_s-\alpha_0)}{\alpha_s-2\alpha_0}At. \qquad (52)$$

The settling process is terminated at time $t = t_s$ when the liquid–suspension interface meets the horizontal part of the suspension–sediment interface. Hence $t_s$ is given by the relation $z_0(t_s)+At_s = 1$.

Finally the streamfunctions $\psi_1$ and $\psi_2$, describing fluid streamlines $\psi_1 = \text{const}$ and particle streamlines $\psi_2 = \text{const}$, respectively, can be found in the same manner as in § 5.1. The result is

$$\psi_{1,2} = \frac{f(\alpha_0)}{\tan\theta}\left[\left(n\frac{1-z-At}{a'-At}\mp 1\right)x' - n\frac{(1-z-2At)z}{a'-At}\right], \qquad (53)$$

where, for $\psi_1$, $n = (1-\alpha_0)/\alpha_0$ and the upper sign is taken, whereas, for $\psi_2$, $n = 1$ and the lower sign is taken.

The results become rather simple for very dilute suspensions, i.e. $\alpha_0 \ll 1$. Since $f(\alpha_0)\rightarrow\alpha_0$ as $\alpha_0\rightarrow 0$ we obtain from (50)–(53) the following limiting results as $\alpha_0\rightarrow 0$:

$$j_z = (1-z)/a', \quad j_x\tan\theta = (1-2z+x')/a', \qquad (54)$$

$$z_0 = (1+a')(1-e^{-t/a'}), \qquad (55)$$

$$t_s = a'\ln(1+1/a'), \qquad (56)$$

$$\psi_1 a\tan^2\theta = (1-z)(x'-z), \qquad (57a)$$

$$(\psi_2/\alpha_0)a\tan^2\theta = x'(1+a'-z)-(1-z)z. \qquad (57b)$$

Equations (55) and (56) are in agreement with the results of Ponder (1925) and Nakamura & Kuroda (1937). According to (54) and (57$a,b$) the velocities and streamlines within the suspension region are independent of time (but, of course, the boundaries of this region move with time). Thus particle streamlines and particle paths are identical in the limiting case $\alpha_0\rightarrow 0$. Note, furthermore, that in the reduced co-ordinate system $(x', z)$ (with $x' = (x+a)\tan\theta$) the streamlines do not depend separately on the two geometrical parameters $a$ and $\theta$, but only on the combined parameter $a' = a\tan\theta$. A typical example is shown in figure 8.

Retaining only first-order quantities in terms of the small initial concentration $\alpha_0$ also simplifies (46)–(49), which give the height of the sediment layer. The height distribution after termination of the settling process may be of particular interest. With $t = t_s$ according to (56), we obtain from (46$a$) for the sediment-layer height above the horizontal bottom

$$s = \frac{\alpha_0}{\alpha_s}a'\ln\frac{1+a'}{a'}, \qquad (58a)$$

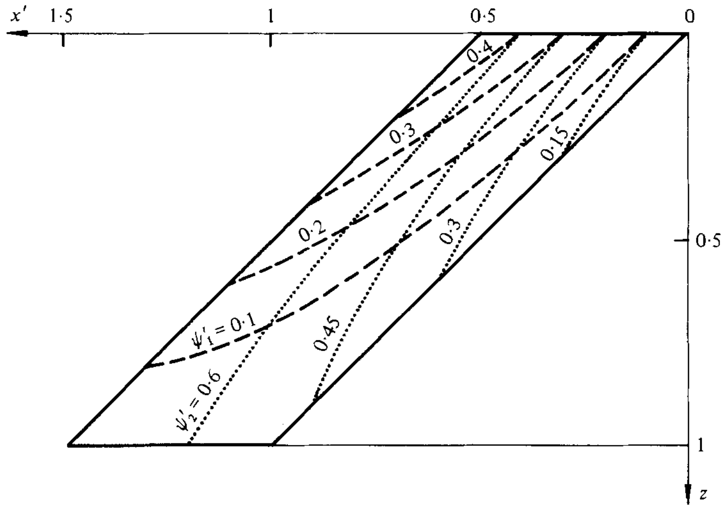


FIGURE 8. Streamlines (paths) of liquid (– – – –) and particles (......) in a vessel with parallel, inclined plane walls. Very dilute initial suspension ($\alpha_0 \to 0$); $a' = a \tan\theta = \frac{1}{2}$; $x' = (x+a)\tan\theta$, $\psi_1' = \psi_1 a \tan^2\theta$, $\psi_2' = (\psi_2/\alpha_0)\, a \tan^2\theta$.

and from (46*b*) for the sediment-layer height above the inclined wall

$$s = \frac{\alpha_0}{\alpha_s} a' \ln \frac{1+a'}{1+a'-x'} \quad (x' \leqq 1). \tag{58b}$$

This work was supported by the Fonds zur Förderung der wissenschaftlichen Forschung, Projekt Nr. 4078. The author is grateful to Professor Batchelor and to the referees for valuable comments and suggestions.

## Appendix: The flow in the boundary layer at a downward-facing inclined wall

For simplicity only two-dimensional and axisymmetric flows are considered in what follows. Boundary-layer co-ordinates $(\xi, \eta)$ are used, and the $\xi$- and $\eta$-components of the total volume flux **j** are denoted respectively by $u$ and $v$ (figure 9). Note that in the clear liquid ($\alpha = 0$) $u$ and $v$ are identical with the velocity components.

*The inviscid part of the boundary layer*

The following stretched variables are defined:

$$\left.\begin{aligned} &\tilde{u} = G^{-\frac{1}{2}} R u, \quad \tilde{v} = v, \\ &\tilde{\xi} = \xi, \quad \tilde{\eta} = G^{\frac{1}{2}} R^{-1} \eta, \quad \tilde{\delta} = G^{\frac{1}{2}} R^{-1} \delta. \end{aligned}\right\} \tag{A 1}$$

The equation of the interface between the suspension and the clear liquid is $\tilde{\eta} = \tilde{\delta}(\tilde{\xi}, t)$.

Considering the limit $G/R^2 \to \infty$ and $G/R^4 \to 0$, the equation of motion of the liquid in the direction normal to the wall reduces to $\partial P/\partial \tilde{\eta} = 0$. Thus the pressure in the particle-free layer is equal to that in the suspension and given by (5). As $\alpha = 0$ in the particle-free layer, the equation of motion in the tangential direction becomes

$$\tilde{u}\frac{\partial \tilde{u}}{\partial \tilde{\xi}} + \tilde{v}\frac{\partial \tilde{u}}{\partial \tilde{\eta}} = \frac{\alpha(z,t)}{\alpha_0} \sin\theta. \tag{A 2}$$

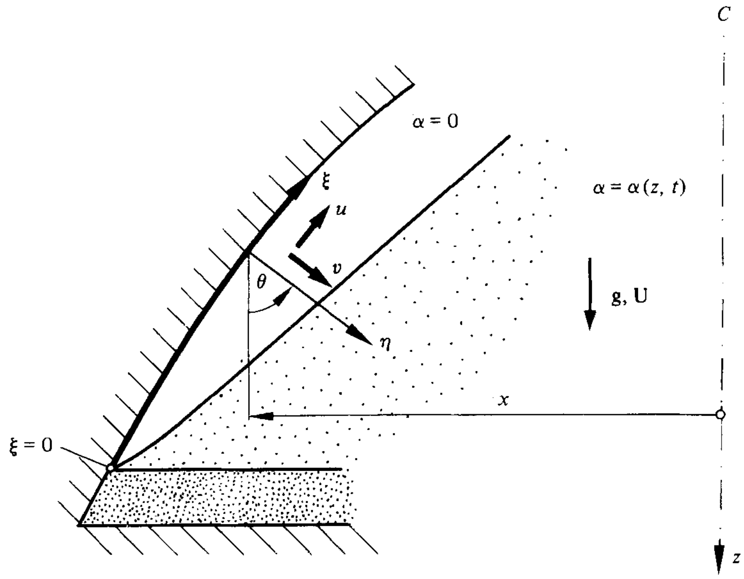


FIGURE 9. Boundary layer at downward-facing inclined wall.

This equation shows that, in a first approximation, the flow in the boundary layer of clear liquid is inviscid and quasi-steady. The concentration $\alpha(z,t)$ in the suspension is to be determined by solving the kinematic-wave problem formulated in §§2–4.

The continuity equation can be written as

$$\frac{\partial(x^\sigma \tilde{u})}{\partial \tilde{\xi}} + \frac{\partial(x^\sigma \tilde{v})}{\partial \tilde{\eta}} = 0, \tag{A 3}$$

where an integer $\sigma$ is used to distinguish the two-dimensional case ($\sigma = 0$) from the axisymmetric case ($\sigma = 1$), and $x$ is the distance of a point at the wall from the axis of symmetry (figure 9). The appropriate boundary conditions are

$$\tilde{v} = 0 \quad \text{at} \quad \tilde{\eta} = 0, \tag{A 4a}$$

$$\tilde{v} = j_n \quad \text{at} \quad \tilde{\eta} = \tilde{\delta}(\tilde{\xi}, t), \tag{A 4b}$$

$$\tilde{u} = 0 \quad \text{at} \quad \tilde{\eta} = \tilde{\delta}(\tilde{\xi}, t). \tag{A 4c}$$

Equation (A 4$b$) expresses the continuity of the total flux at the suspension–liquid interface. With $j_n$ given by (21) it is guaranteed that no particles flow through the interface ($j_{2n} = 0$). Equation (A 4$c$) is a consequence of the conservation of tangential momentum flux through the interface, together with the fact that the tangential velocity in the suspension is an order of magnitude smaller than in the particle-free boundary layer.

The continuity equation (A 3) can be satisfied by introducing a streamfunction $\psi$ as follows:

$$\left.\begin{aligned} \tilde{u} &= \frac{1}{x^\sigma}\frac{\partial(x^\sigma \psi)}{\partial \tilde{\eta}} = \frac{\partial \psi}{\partial \tilde{\eta}}, \\ \tilde{v} &= -\frac{1}{x^\sigma}\frac{\partial(x^\sigma \psi)}{\partial \tilde{\xi}} = -\frac{\partial \psi}{\partial \tilde{\xi}} + \frac{\sigma \cos\theta}{x}\psi. \end{aligned}\right\} \tag{A 5}$$

Substituting into the momentum equation (A 2) yields

$$\psi_{\tilde{\eta}}\psi_{\tilde{\xi}\tilde{\eta}}-\left(\psi_{\tilde{\xi}}-\frac{\sigma\cos\theta}{x}\psi\right)\psi_{\tilde{\eta}\tilde{\eta}}=\frac{\alpha(z,t)}{\alpha_0}\sin\theta, \tag{A 6}$$

where partial derivatives with respect to $\tilde{\xi}$ and $\tilde{\eta}$ are denoted by subscripts $\tilde{\xi}$ and $\tilde{\eta}$ respectively. The boundary conditions in terms of $\psi$ read

$$\psi = 0 \quad \text{at} \quad \tilde{\eta} = 0; \tag{A 7a}$$

$$\psi_{\tilde{\xi}}-\frac{\sigma\cos\theta}{x}\psi=\frac{f(\alpha)}{\alpha}\cos\theta \quad \text{at} \quad \tilde{\eta}=\tilde{\delta}(\tilde{\xi},t); \tag{A 7b}$$

$$\psi_{\tilde{\eta}} = 0 \quad \text{at} \quad \tilde{\eta}=\tilde{\delta}(\tilde{\xi},t). \tag{A 7c}$$

Of course, the inviscid boundary-layer flow can neither satisfy the condition of zero velocity at the wall nor will the shear stress be continuous at the suspension–liquid interface. Hence a viscous sublayer at the wall and a free shear layer at the interface have to be introduced. Both layers are very thin in comparison with the inviscid part of the boundary layer.

*The viscous sublayer at the wall*

The convective, buoyancy and viscous terms become of equal importance if the variables are stretched as follows:

$$\left.\begin{aligned} u_s &= G^{-\frac{1}{2}}Ru, \quad v_s = G^{-\frac{1}{4}}Rv,\\ \xi_s &= \xi, \quad \eta_s = G^{\frac{1}{4}}\eta. \end{aligned}\right\} \tag{A 8}$$

Thus the ratio of the sublayer thickness to the total boundary-layer thickness is as small as $G^{\frac{1}{4}}R^{-1}$.

Written in the sublayer variables defined by (A 8), the momentum equation becomes

$$u_s\frac{\partial u_s}{\partial \xi_s}+v_s\frac{\partial u_s}{\partial \eta_s}=\frac{\alpha(z,t)}{\alpha_0}\sin\theta+\frac{\partial^2 u_s}{\partial \eta_s^2}. \tag{A 9}$$

The continuity equation (A 3) remains unchanged, i.e. the tilde is to be replaced by the subscript s. The boundary and matching conditions are

$$u_s = v_s = 0 \quad \text{at} \quad \eta_s = 0, \tag{A 10a}$$

$$\lim_{\eta_s\to\infty} u_s = \lim_{\tilde{\eta}\to 0}\tilde{u}. \tag{A 10b}$$

Obviously the problem defined for the sublayer is of the type of a classical viscous boundary layer.

*The free shear layer at the interface*

Since the normal velocity $v$ is equal to $j_n(\xi)$ on both sides of the suspension–liquid interface, $v$ will be only weakly disturbed in the free shear layer. As $j_n = O(1)$, the viscous term $R^{-1}\partial^2u/\partial\eta^2$ can balance the convective term $v\,\partial u/\partial\eta$ only if the layer thickness is as small as $R^{-1}$. (This is much smaller than the thickness of the viscous sublayer at the wall.) As far as the order of magnitude of the tangential velocity in the free shear layer is concerned we have to make sure that matching can be accomplished with $u = O(1)$ in the bulk of the suspension and with $\partial u/\partial \eta = O(G/R^2)$ in the particle-free boundary layer. This requires the following stretched variables:

$$\xi_F = \xi, \quad \eta_F = R(\eta - \delta), \tag{A 11}$$

$$u_F = u, \quad v_F = R[v - j_n(\xi)] \quad \text{if} \quad G/R^3 = O(1) \quad \text{or} \quad G/R^3 \to 0, \tag{A 12a}$$

$$u_F = (R^3/G)\,u, \quad v_F = (R^4/G)\,[v - j_n(\xi)] \quad \text{if} \quad G/R^3 \to \infty. \tag{A 12b}$$

As before, $j_n(\xi)$ is given by (21). In the case $G/R^3 = O(1)$ or $G/R^3 \to 0$ the tangential velocity in the free shear layer is of the order of unity, i.e. of the same order of magnitude as the drift flux. This requires taking the relative motion into account in the momentum equation, but it cannot be done rigorously by applying the relation (7) since the drift-flux model is based on neglecting inertial terms in the momentum equation (cf. Wallis 1969, pp. 91 and 123). We shall therefore consider the case $G/R^3 \to \infty$ in which the drift flux is negligible in the tangential motion of the mixture. Since there is no influence of the free shear layer on the leading approximation of the flow outside of it, the condition $G/R^3 \to \infty$ applies to the free shear layer only.

It then follows, from the continuity equation (11) for the particles, that $\partial\alpha/\partial\eta_F = 0$. This yields

$$\left.\begin{aligned} \alpha &= 0 \quad (\eta_F < 0), \\ \alpha &= \alpha(z,t) \quad (\eta_F > 0); \end{aligned}\right\} \tag{A 13}$$

i.e. the result that the particle concentration in the suspension does not vary in horizontal direction remains true even in the free shear layer.

The equation of continuity of the mixture, (A 3), is again reproduced with tilde replaced by the subscript F. Taking (A 13) into account, the tangential momentum equation becomes

$$\left.\begin{aligned} j_n \frac{\partial u_F}{\partial \eta_F} &= \frac{\alpha}{\alpha_0}\sin\theta + \frac{\partial^2 u_F}{\partial \eta_F^2} \quad (\eta_F < 0), \\ j_n \frac{\partial u_F}{\partial \eta_F} &= \frac{\nu_\alpha}{\nu_1}\frac{\partial^2 u_F}{\partial \eta_F^2} \quad (\eta_F > 0), \end{aligned}\right\} \tag{A 14}$$

where $\nu_\alpha$ is the kinematic viscosity of the suspension with particle concentration $\alpha$. It is related to the dynamic viscosity $\mu_\alpha$ of the suspension by $\nu_\alpha = \mu_\alpha/\rho_\alpha$ with

$$\rho_\alpha = (1-\alpha)\rho_1 + \alpha\rho_2.$$

The matching conditions are

$$\lim_{\eta_F \to -\infty} \frac{\partial u_F}{\partial \eta_F} = \frac{\alpha \sin\theta}{\alpha_0 j_n}, \tag{A 15a}$$

$$\lim_{\eta_F \to +\infty} u_F = 0. \tag{A 15b}$$

The right-hand side of (A 15a) is the value of $\partial\tilde{u}/\partial\tilde{\eta}$ at $\tilde{\eta} = \tilde{\delta}$, as obtained from the inviscid momentum equation (A 2) together with the boundary conditions (A 4b, c).

At the interface between the suspension and the clear liquid it is required that the total volume flux and the shear stress be continuous. This yields the boundary conditions

$$\left.\begin{aligned} \lim_{\eta_F \to 0-} \left(\mu_1 \frac{\partial u_F}{\partial \eta_F}\right) &= \lim_{\eta_F \to 0+} \left(\mu_\alpha \frac{\partial u_F}{\partial \eta_F}\right), \\ \lim_{\eta_F \to 0-} u_F &= \lim_{\eta_F \to 0+} u_F, \\ \lim_{\eta_F \to 0-} v_F &= \lim_{\eta_F \to 0+} v_F = 0. \end{aligned}\right\} \tag{A 16}$$

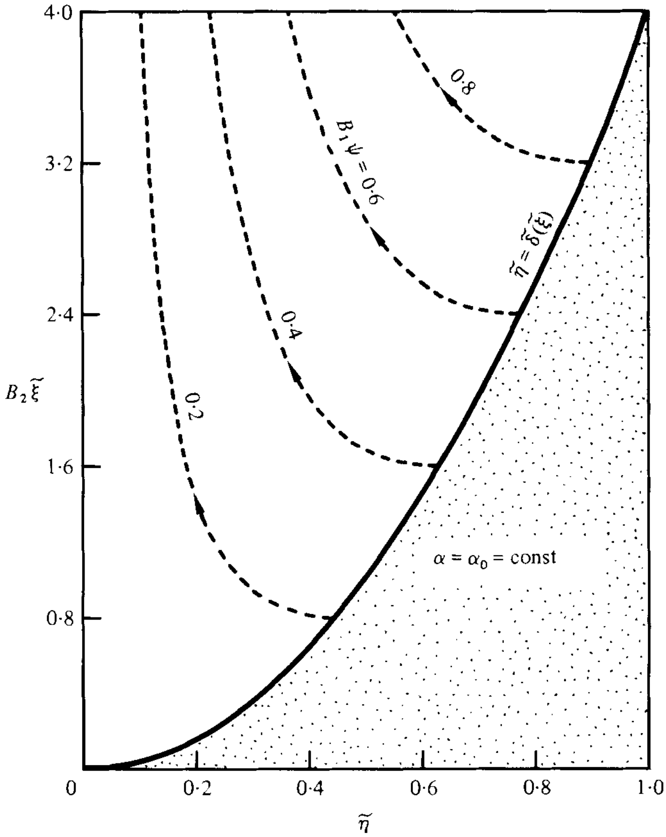


FIGURE 10. Streamlines $\psi(\tilde{\xi}, \tilde{\eta}) = \text{const}$ in the particle-free boundary layer at a plane inclined wall; $B_1 = 2f(\alpha_0)/\alpha_0 \tan\theta$, $B_2 = 2B_1^2 \sin\theta$.

The solution of (A 14) subject to the auxiliary conditions (A 15$a,b$) and (A 16) is found to be

$$\left.\begin{aligned} u_F &= \left(\eta_F + \frac{\rho_1}{\rho_\alpha}\frac{1}{\dot{j}_n}\right)\frac{\alpha\sin\theta}{\alpha_0 \dot{j}_n} \quad (\eta_F < 0), \\ u_F &= \frac{\rho_1 \alpha \sin\theta}{\rho_\alpha \alpha_0 \dot{j}_n^2}\exp\left(\frac{\nu_1 \dot{j}_n}{\nu_\alpha}\eta_F\right) \quad (\eta_F > 0). \end{aligned}\right\} \qquad \text{(A 17)}$$

As was to be expected, (A 17) shows that $u_F > 0$, i.e. the motion in the free shear layer is directed upwards.

*Example*

For a plane wall ($\sigma = 0$) and a sedimentation process of type I ($\alpha = \alpha_0 = \text{const}$), the equations of the inviscid boundary-layer flow of clear liquid, i.e. (A 6) and (A 7$a$–$c$), possess the similarity solution

$$\left.\begin{aligned} \psi &= \tilde{\xi}\left[(2\sin\theta)^{\frac{1}{2}}\lambda - \frac{\alpha_0 \tan\theta}{2f(\alpha_0)}\lambda^2\right], \\ \lambda &= \tilde{\eta}\tilde{\xi}^{-\frac{1}{2}}, \\ \tilde{\delta} &= \frac{(2\sin\theta)^{\frac{1}{2}}}{\tan\theta}\frac{f(\alpha_0)}{\alpha_0}\tilde{\xi}^{\frac{1}{2}}. \end{aligned}\right\} \qquad \text{(A 18)}$$

Note that the origin of the boundary-layer co-ordinates is at the intersection of the sediment surface and the wall (figure 9).

Representative streamlines are shown in figure 10. The variables are stretched such that the streamline pattern is independent of both the inclination angle $\theta$ and the initial concentration $\alpha_0$.

It follows from (A 5) and (A 18) that both the tangential and normal velocity components are linearly distributed across the boundary layer, with

$$\left.\begin{aligned} \tilde{u} &= (2\sin\theta)^{\frac{1}{2}}\tilde{\xi}^{\frac{1}{3}}, \quad \tilde{v} = 0 \quad \text{at} \quad \tilde{\eta} = 0, \\ \tilde{u} &= 0, \quad \tilde{v} = -[f(\alpha_0)/\alpha_0]\cos\theta \quad \text{at} \quad \tilde{\eta} = \tilde{\delta}. \end{aligned}\right\} \qquad (A\ 19)$$

As the tangential velocity of the inviscid flow at the wall is proportional to $\tilde{\xi}^{\frac{1}{3}}$, the viscous-sublayer flow is analogous to the classical boundary-layer flow at a wedge with 60° angle of attack. The Falkner–Skan equation, however, is to be modified slightly owing to the buoyancy term on the right-hand side of (A 9).

## REFERENCES

ACRIVOS, A. & HERBOLZHEIMER, E. 1979 Enhanced sedimentation in settling tanks with inclined walls. *J. Fluid Mech.* **92**, 435–457.

ANESTIS, G. 1981 Eine eindimensionale Theorie der Sedimentation in Absetzbehältern veränderlichen Querschnitts und in Zentrifugen. Dissertation, Techn. Univ. Wien.

BARON, G. & WAJC, S. 1979 Behinderte Sedimentation in Zentrifugen. *Chem. Ing. Tech.* **51**, 333.

BOYCOTT, A. E. 1920 Sedimentation of blood corpuscles. *Nature* **104**, 532.

HAYES, W. D. 1974 Introduction to wave propagation. In *Nonlinear Waves* (ed. S. Leibovich & A. R. Seebass), pp. 1–43. Cornell University Press.

HERBOLZHEIMER, E. & ACRIVOS, A. 1981 Enhanced sedimentation in narrow tilted channels. *J. Fluid Mech.* **108**, 485–499.

HILL, W. D., ROTHFUS, R. R. & LI, K. 1977 Boundary-enhanced sedimentation due to settling convection. *Int. J. Multiphase Flow* **3**, 561–583.

KLUWICK, A. 1977 Kinematische Wellen. *Acta Mechanica* **26**, 15–46.

NAKAMURA, H. & KURODA, K. 1937 La cause de l'accélération de la vitesse de sédimentation des suspensions dans les récipients inclinés. *Keijo J. Med.* **8**, 256–296.

PONDER, E. 1925 On sedimentation and rouleaux formation. *Quart. J. Exp. Physiol.* **15**, 235–252.

RICHARDSON, J. F. & ZAKI, W. N. 1954 Sedimentation and fluidisation: Part I. *Trans. Inst. Chem. Engrs* **32**, 35–53.

SHANNON, P. T., DEHAAS, R. T., STROUPE, E. P. & TORY, E. M. 1964 Batch and continuous thickening – prediction of batch settling behavior from initial rate data with results for rigid spheres. *I & EC Fundamentals* **3**, 250–260.

SHANNON, P. T. & TORY, E. M. 1965 Settling of slurries. *Ind. Engng Chem.* **57**, 18–25.

WALLIS, G. B. 1969 *One-dimensional Two-phase Flow.* McGraw-Hill.

WHITHAM, G. B. 1974 *Linear and Nonlinear Waves.* Wiley.